

---

# STABILITY ANALYSIS OF A MODIFIED LESLIE–GOWER PREDATION MODEL WITH WEAK ALLEE EFFECT ON THE PREY

---

**Claudio Arancibia–Ibarra**

School of Mathematical Sciences, Queensland University of Technology  
GPO Box 2434, GP Campus, Brisbane, Queensland 4001 Australia  
Facultad de Ingeniería y Negocios, Universidad de Las Américas  
Av. Manuel Montt 948, Santiago, Chile  
claudio.arancibia@hdr.qut.edu.au

**José Flores**

Department of Mathematics, The University of South Dakota (USD)  
Vermillion, South Dakota, USA  
Jose.Flores@usd.edu

June 5, 2022

## ABSTRACT

In this manuscript, we study predator-prey model in which the prey population is affected by a density-dependent phenomenon or weak Allee effect. In particular, we study the behaviour on the Leslie–Gower predator-prey model with a hyperbolic functional response and weak Allee effect. These results reveal that the model support the coexistence and/or the oscillation of both predator and prey populations. From our results, we identify regions in parameter space in which the system presents separatrix curves which divide the behaviour of the trajectories, a homoclinic curve generated by the stable and unstable manifolds of a positive equilibrium point and different kinds of bifurcations, such as saddle-node bifurcations, Hopf bifurcations, Bogadonov–Takens bifurcations and homoclinic bifurcations. We also show that solutions are highly sensitive to initial conditions.

**Keywords** Leslie–Gower model · weak Allee effect · Holling type II · bifurcations · numerical simulation.

## 1 Introduction

The dynamics of predator-prey models are becoming increasingly important in mathematics [1, 2, 3] and ecology [4, 5, 6, 7]. The goal of these studies is to describe and analyse the predation interaction between the predator and the prey to predict how they respond to further interventions [8, 9]. Current dynamics studies often use mathematical models to describe the species' interactions and the time-series behaviours [10, 11]. These mathematical models aim to be representative of real natural phenomena capturing the essentials of the dynamics. New technology has been used to study biological and physical phenomenon revealing that species' interactions are more complex than previous analysis in this field [12, 13, 14, 7]. The importance of these phenomenas are becoming increasingly apparent as research findings have shown that ecosystem dynamics depend on the particular nature of interaction processes, such as the functional response or predation rate [15, 6, 7, 16].

The standard approach for using models to understand ecological systems is to design a framework based on simple principles and compare species' abundance time-series that result from the predicting analysis from those models. However, this approach becomes more difficult when additional nuances to standard models are added, making them more complex and difficult to parameterise. For instance, Graham and Lambin [17] showed that field-vole (*Microtus agrestis*) survival can be affected by reducing least weasel (*Mustela nivalis*) predation. The authors in [17] also demonstrated that weasels were suppressed in summer and autumn, while the vole (*Microtus agrestis*) population always declined to low density. However, the authors in [17] argued that the underlying model was difficult to study due to a large number of parameters. Several ecologists have

attempted to solve this issue by applying qualitative approaches, making few assumptions about the models' functional forms or parameters [18, 19, 20].

The Leslie–Gower predator-prey model [9] is given by

$$\begin{aligned}\frac{dN}{dt} &= rN \left(1 - \frac{N}{K}\right) - \frac{qNP}{N+a}, \\ \frac{dP}{dt} &= sP \left(1 - \frac{P}{hN}\right).\end{aligned}\tag{1}$$

Where  $N(t)$  and  $P(t)$  are used to represent the size of the prey population at time  $t$  respectively,  $r$  and  $s$  are the intrinsic growth rate for the prey and predator respectively,  $h$  is a measure of the quality of the prey as food for the predator,  $K$  is the prey environmental carrying capacity,  $q$  is the maximum predation rate per capita and  $a$  is half of the saturated response level [7]. The growth of the predator and prey population is a logistic form and the predator environmental carrying capacity is a prey dependant. Note that in this manuscript we will use a type II functional response, i.e.  $H(N) = qN/(N+a)$  [21].

In population dynamics, many ecological mechanisms are connected with individual cooperation such as strategies to hunt, collaboration in unfavourable abiotic conditions and reproduction [22]. When the predator population density is low they might have, per capita, more resources and benefits. However, there are species that may suffer from a lack of conspecifics, which may impact their reproduction, or reduce their probability to survive, when their population density is low. The Allee effect is defined as the relation between population size and fitness. The lower the population size, the lower the fitness [23, 24, 25]. Additionally, the Allee effect appears in some populations due to the density-dependent habitat selection [26].

Individuals of many species use cooperative strategies to hunt or distract predators, seek food together, join forces to survive in unfavourable abiotic conditions, or simply seek sexual reproduction at the same time and/or place [24]. Individuals may be less likely to reproduce or survive in a small-sized population [25]. In these instances, the size of the population is relatively important, as for a smaller size of biomass adaptability may be diminished [27]. When Allee analysed the data of the false weevil (*Tribolium confusum*) he observed that the highest growth rates of their populations per capita were at intermediate densities [27]. The fact that they were lower in high densities was not surprising, as intraspecific competition is high. When fewer males were present, females produced fewer eggs, which is not an obvious correlation for an insect. In this case, optimal egg production was thus achieved at intermediate densities. In most predation models, the Allee effect is considered to influence the population of prey and this effect is independent of the type of functional response or rate of consumption that expresses the change of predation with the size of the population of prey. For instance, Ostfeld and Canhan [28] found that the stabilisation of vole (*Microtus agrestis*) populations in southeastern New York depends on the variation in reproductive rate and recruitment of the population. This effect is referred to as Allee effect [24]. To incorporate the Allee effects in (1)  $r(1 - N/K)$  is replaced by  $r(1 - N/K)(N - m)$  where  $m$  is the Allee threshold. Moreover, for  $0 < m < K$ , the per-capita growth rate of the prey population with the Allee effect included is negative, but increasing, for  $N \in [0, m)$ , and this is referred to as the strong Allee effect. When  $m \leq 0$ , the per-capita growth rate is positive but increases at low prey population densities and this is referred to as the weak Allee effect [24, 27].

With an Allee effect included, the Leslie–Gower predator-prey model (1) becomes

$$\begin{aligned}\frac{dN}{dt} &= rN \left(1 - \frac{N}{K}\right) (N - m) - \frac{qNP}{N+a} = N \cdot W(N, P), \\ \frac{dP}{dt} &= sP \left(1 - \frac{P}{hN}\right) = P \cdot R(N, P).\end{aligned}\tag{2}$$

The aim of this manuscript is to study the Leslie–Gower predator-prey model with weak Allee effect on prey, that is (2) with  $m < 0$ . We complement the results of Ostfeld and Canhan [28] where the authors studied the stabilisation of file-vole population which depends on the variation in reproductive rate and recruitment of the population (Allee effect). File-vole specie also depends on the survival rate for adults were delayed density-dependent (weak Allee effect). On the other hand, we observe that the main difference between system (1) and (2) with  $m < 0$  is the fact that (2) has at most three positive equilibrium points in the first quadrant instead of one for system (1) and two for system (2) and  $m \leq 0$  [29, 30, 31]. This additional equilibrium points gives rise to different type of bifurcations such as saddle-node bifurcation, Bogadonov–Takens bifurcation, and homoclinic bifurcation. This manuscript also extends some of the results obtained by Arancibia–Ibarra and González–Olivares [30] and González–Olivares *et al.* [31] for a modified Leslie–Gower model with  $m = 0$ , that is, with a specific type of weak Allee effect. The authors showed the existence of a stable limit cycle which represent the oscillation of both populations.

The Leslie–Gower models with strong Allee effect in the prey and different type of functional responses have been extensible studied in [32, 33]. In these articles the authors showed that the system, for certain system parameters, can have the extinction of both species and it also support the stabilisation of both population over the time. Moreover, system (2) with  $m < 0$  complement the results of the Leslie–Gower model studied by Courchamp *et al.* [27] in which the prey is affected a density-dependent

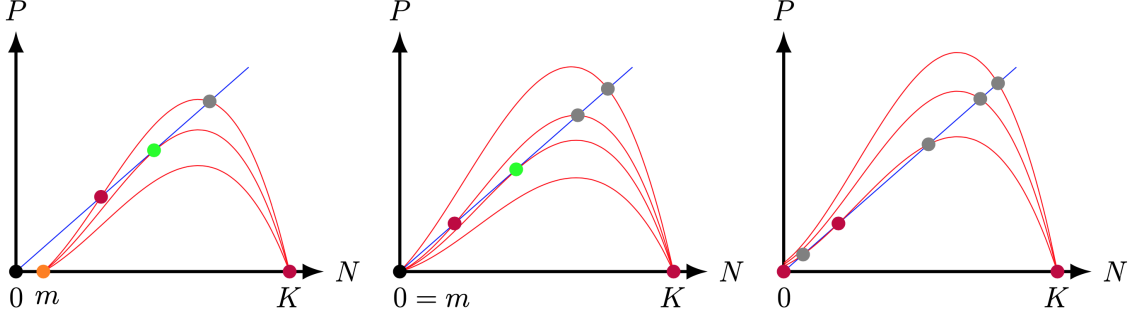


Figure 1: The intersection of the predator nullcline (blue curve) and the prey nullcline (red curve) in system (2) with strong Allee effect ( $m > 0$ ) in the left panel, weak Allee effect ( $m = 0$ ) in the middle panel and weak Allee effect ( $m < 0$ ) in the right panel. Note that the number of positive equilibrium points is given by changing the predation rate per capita  $q$ . The purple circle represent a saddle equilibrium point, the grey circle represent an equilibrium point which can be stable or unstable, the black circle represent an equilibrium point which is always stable, the orange circle represent an equilibrium point which is always unstable and the green circle represent an equilibrium point which is the collision of two equilibrium points.

phenomenon. We will show the impact in the basin of attraction by considering a weak Allee effect in the prey for two parameters which are the rescaled intrinsic growth rate of the predator and the predation rate.

The Leslie–Gower model with weak Allee effect is presented in Section 2. The main properties of the Leslie–Gower model are studied in Section 3. In which we study the stability of the equilibrium points and present the conditions for which the model undergoes to a different type of bifurcations. Finally, in 4 we summarise the results and discuss the ecological implications of the model.

## 2 The Model

The Leslie–Gower model with weak Allee effect is given by (2) with  $m < 0$ , and we only consider the model in the domain  $\Omega = \{(N, P) \in \mathbb{R}^2, N > 0, P \geq 0\}$  and  $(r, K, q, a, s, h) \in \mathbb{R}_+^6, m < 0$  and  $a < K$ . As system (2) is of Kolmogorov type [34] since  $dN/dt = N \cdot W(N, P)$  and  $dP/dt = P \cdot R(N, P)$ . That is, the axes are invariant. The positive equilibrium points of the system<sup>1</sup> (2) are  $(K, 0)$  and  $(x^*, y^*)$  which is the intersection of the nullclines

$$P = hN \quad \text{and} \quad P = \frac{r}{q} \left(1 - \frac{N}{K}\right) (N + a) (N - m).$$

Note that, system (2) can have at most three positive equilibrium points in  $\Omega$ . In contrast, system (2) with  $m \geq 0$  can have at most two positive equilibrium points in the same domain  $\Omega$  [29, 31, 35], see Figure 1.

In order to simplify the analysis we follow the nondimensionalisation approach studied in [29] where the author introduce the dimensionless variables  $(u, v, \tau)$  given by

$$\varphi : \bar{\Omega} \times \mathbb{R} \rightarrow \Omega \times \mathbb{R} \quad \text{where} \quad \varphi(u, v, \tau) = \left( \frac{N}{K}, \frac{P}{hK}, \frac{rKt}{u \left(u + \frac{a}{K}\right)} \right). \quad (3)$$

The authors set  $A := a/K \in (0, 1)$ ,  $S := s/(rK)$ ,  $Q := hq/(rK)$  and  $M := m/K$ , then (2) transform into the nondimensionalised system

$$\begin{aligned} \frac{du}{d\tau} &= u^2 ((u + A) (1 - u) (u - M) - Qv), \\ \frac{dv}{d\tau} &= S(u + A) (u - v) v. \end{aligned} \quad (4)$$

Additionally, the authors studied system (4) in  $\bar{\Omega} = \{(u, v) \in \mathbb{R}^2, u > 0, v \geq 0\}$  and they proved that  $\varphi$  (3) is a diffeomorphism which preserve the orientation of time [36, 37]. The  $u$ -nullclines of system (4) are given by  $u = 0$  and  $v = (u + A) (1 - u) (u - M) / Q$ , while the  $v$ -nullclines are given by  $v = 0$  and  $v = u$ . Hence, the equilibrium point of

<sup>1</sup>In this manuscript, we will refer to an equilibrium point as with two positive entries as a positive equilibrium point.

Cases	$T(A, M)$	$L(A, M, Q)$	Positive solution(s) of equation (5)
I	$\leq 0$	$\mathbb{R}$	1 (see Lemma 3.1)
II	$> 0$	$\geq 0$	1 (see Lemma 3.1)
III	$> 0$	$< 0$	3 (see Lemmas 3.2, 3.3 and 3.4)

Table 1: Sign of the coefficient and number of positive solution(s) of equation (5). Here,  $T(A, M) = 1 - A + M$ ,  $L(A, M, Q) = A(M + 1) - Q - M$  and  $M < 0$ .

system (4) are  $(0, 0)$ ,  $(1, 0)$ , and the positive equilibrium point(s)  $(u^*, v^*)$  with  $v^* = u^*$  and where  $u^*$  is determined by the solution(s) of

$$u^3 - T(A, M)u^2 - L(A, M, Q)u + AM = 0, \quad (5)$$

with  $T(A, M) = 1 - A + M$  and  $L(A, M, Q) = A(M + 1) - Q - M$ . We analyse the numbers of positive solution(s) of the equation (5) by using the Descartes signs rule. Therefore, we obtain nine cases of positive solution(s) of equation (5) which are presented in Table 1.

We can conclude from Table 1 that equation (5) can always have one positive root, we will denote it by  $u_1 > 0$ . Due to the difficult to determine the exact solutions of equation (5), we divide equation (5) by  $(u - u_1)$ . Therefore, we obtain a second degree equation given by

$$u^2 + u(u_1 - T(A, M)) + u_1(u_1 - T(A, M)) - L(A, M, Q) = 0, \quad (6)$$

it follows that

$$u_1(u_1(u_1 - T(A, M)) - L(A, M, Q)) + AM = 0 \text{ and } Q = \frac{1}{u_1}(1 - u_1)(u_1 - M)(A + u_1).$$

We describe the case when  $T(A, M) > 0$  and  $L(A, M, Q) < 0$  for the solution of equation (6) and hence the number of positive equilibrium points. Therefore, the solution of equation (6) are:

$$u_2 = \frac{1}{2} \left( T(A, M) - u_1 - \sqrt{\Delta} \right), \quad u_3 = \frac{1}{2} \left( T(A, M) - u_1 + \sqrt{\Delta} \right) \text{ and} \quad (7)$$

$$\Delta = (u_1 - T(A, M))^2 - 4(u_1(u_1 - T(A, M)) - L(A, M, Q)).$$

In particular,

- (i) if  $\Delta < 0$  (7), then (4) has one positive equilibrium point in the first quadrant  $P_1$ ;
- (ii) if  $\Delta > 0$  (7), then (4) has three positive equilibrium points  $P_i = (u_i, u_i)$ , with  $i = 1, 2, 3$ , in the first quadrant; and
- (iii) if  $\Delta = 0$  (7), then (4) has two positive equilibrium points with one of them is order two.

Note that if  $\Delta = 0$  (7), then two positive equilibrium points collapses, i.e  $P_1 = P_2$  or  $P_2 = P_3$  or  $P_1 = P_3$ , see Figure (2). We also observe that none of these equilibrium points explicitly depend on the system parameter  $S$ . Therefore,  $S$  and  $Q$  are the natural candidates to act as bifurcation parameters. Moreover, if we assume that  $Q$  is such that  $\Delta > 0$ ,  $T(A, M) > 0$  and  $L(A, M, Q) < 0$  then in Figure (2) we observe that the equilibrium points  $P_1$ ,  $P_2$  and  $P_3$  can swap the position and thus change from (un)stable node to a saddle point.

In this manuscript we only consider cases (a), (b), (c), (d) and (i), since the other cases presented in Figure (2) have equivalent behaviour.

### 3 Main Results

For system (4) we have the following results.

**Theorem 3.1.** *All solutions of (4) which are initiated in the first quadrant are bounded and eventually end up in  $\Phi = \{(u, v), 0 < u \leq 1, 0 \leq v \leq 1\}$ .*

*Proof.* Arancibia-Ibarra *et al.* proved that all the solution of system (4) with  $M > 0$  are bound and eventually end up in  $\Phi$  [29, Theorem 2]. As all the conditions used to prove Theorem 2 does not depend on the parameter  $M$  we can conclude that for system (4) with  $M < 0$  all the solutions initiated in  $\Omega$  are also bounden and end up in  $\Phi$ .  $\square$

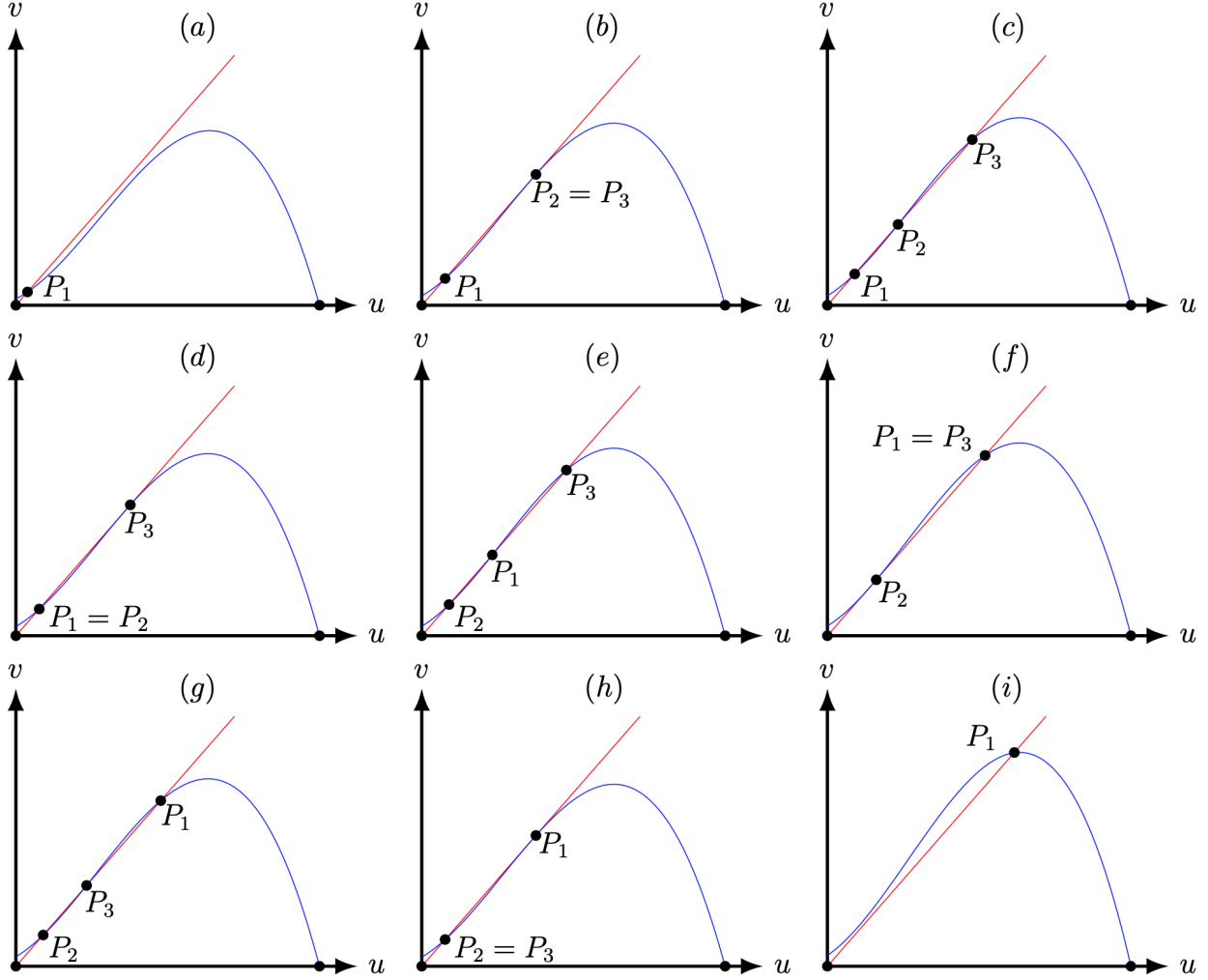


Figure 2: The intersection of the predator nullcline (blue curve) and the prey nullcline (red curve) in system (2) in three points ( $P_1$ ,  $P_2$  and  $P_3$ ) for  $Q$  such that  $\Delta > 0$ ,  $T(A, M) > 0$  and  $L(A, M, Q) < 0$ .

### 3.1 Nature of equilibrium points

To determine the stability of the equilibrium points in the axes  $(0, 0)$ ,  $(M, 0)$  and  $(1, 0)$  we must compute the Jacobian matrix of system (4), that is:

$$J(u, v) = \begin{pmatrix} -uJ_{11} & -Qu^2 \\ Sv(A + 2u - v) & S(u - 2v)(A + u) \end{pmatrix}, \quad (8)$$

with  $J_{11} = 4Au^2 - 4Mu^2 + 2AM - 3Au + 3Mu + 2Qv - 4u^2 + 5u^3 - 3AMu$ . Therefore, the determinant and the trace of the Jacobian matrix (8) are:

$$\begin{aligned} \det(J(u, v)) &= -JSu(u - 2v)(A + u) + QS^2v(A + 2u - v) \text{ and} \\ \text{tr}(J(u, v)) &= -uJ_{11} + S(u - 2v)(A + u) \end{aligned} \quad (9)$$

**Theorem 3.2.** *The equilibrium point  $(0, 0)$  is a non-hyperbolic saddle point and  $(1, 0)$  is a saddle point.*

*Proof.* Stability of the equilibrium point  $(0, 0)$ :

We follow the methodology used to desingularise the origin showed in [29, Lemma 2]. First, we observe that setting  $u = 0$  in system (4) the second equation  $dv/dt = -v^2(SA) < 0$  for  $v \geq 0$ . That is any trajectory starting along the  $v$ -axes converges

to the origin  $(0, 0)$ . Also, the Jacobian matrix,  $J(0, 0)$ , is the zero matrix. Hence the origin  $(0, 0)$  is a non-hyperbolic equilibrium of system (4). Therefore, we will use the *blow-up*<sup>2</sup> method to desingularise the origin and study the dynamics of this equilibrium.

Thus, we consider the vertical *blow-up* given by the transformation

$$(u, v) \rightarrow (xy, y) \quad (10)$$

and the time rescaling

$$\tau \rightarrow \frac{t}{y}. \quad (11)$$

This transformation, (10), is well defined for all values of  $u$  and  $v$  except  $v = 0$  and 'blows-up' the origin of system (4) into the entire  $x$ -axes. Next, our goal is to analyse the equilibria in the positive half axes  $x \geq 0, y = 0$ , in the new system, which is given as follows:

$$\begin{aligned} \frac{dx}{dt} &= x(S(1-x)(A+xy) + x(M-xy)(xy-1)(A+xy) - Qxy) \\ \frac{dy}{dt} &= Sy(x-1)(xy+A) \end{aligned} \quad (12)$$

System (12) has two equilibria in the positive  $x$ -axes of the form  $(x, 0)$  with  $x \geq 0$ . The origin  $O_{xy} = (0, 0)$  and a second equilibrium point  $I_x = (\mu, 0)$  with  $\mu = S/(S+M)$  and  $S > |M|$ . Their corresponding Jacobian matrix  $J_*$  evaluated at  $O_{xy} = (0, 0)$  and  $I_x = (\mu, 0)$  are:

$$J_*(O_{xy}) = \begin{pmatrix} AS & 0 \\ 0 & -AS \end{pmatrix}$$

with eigenvalues  $\lambda_1(O_{xy}) = AS$  and  $\lambda_2(O_{xy}) = -AS$  and

$$J_*(I_x) = \begin{pmatrix} -AS & \frac{S^2(AS(1+M)-Q(M+S))}{(M+S)^3} \\ 0 & -\frac{AMS}{M+S} \end{pmatrix}$$

with eigenvalues  $\lambda_1(I_x) = -AS$  and  $\lambda_2(I_x) = -AMS/(M+S) > 0$ . It follows that  $O_{xy} = (0, 0)$  and  $I_x = (\mu, 0)$  are a saddle in system (4). Moreover, a branch of the unstable manifold  $W^u(I_x)$  of the equilibrium  $I_x = (\mu, 0)$  is in the half-plane  $y > 0$ , as illustrated in the left panel of Figure 3. Furthermore, the other local invariant curves are the axes  $x = 0$  and  $y = 0$ . Hence, taking the inverse of (10), the line  $y = 0$ , including the point  $I_x = (\mu, 0)$ , collapses to the origin  $O_{uv}$  of (4), the line  $x = 0$  is mapped to  $u = 0$  and,  $W^u(I_x)$  is locally mapped to the curve  $\Gamma^u$ . Since the orientation of the orbits in the first quadrant is preserved by (10) and (11), it follows that the origin  $O = (0, 0)$  is a local saddle of (4). The qualitative dynamics in a neighbourhood of the origin  $O_{uv}$  in (4) is illustrated in the right panel of Figure 3.

Stability of the equilibrium point  $(1, 0)$ :

Evaluating the determinant and the trace (9) at the equilibrium point  $(1, 0)$  gives

$$\det(J(1, 0)) = -S(1-M)(A+1)^2 < 0.$$

Therefore, the equilibrium point  $(1, 0)$  is a saddle point, since  $M < 0$ . □

Next, we consider the stability of the positive equilibrium points  $P_{1,2,3}$  of system (4). Note that these equilibrium points are the intersection of the nullcline  $u = v$  such that  $(u+A)(1-u)(u-M) = Qu$ . Therefore, the Jacobian matrix of system (4) becomes

$$J(u, u) = \begin{pmatrix} u^2((1-u)(u-M) - (u+A)(u-M) + (1-u)(u+A)) & -Qu^2 \\ Su(A+u) & -Su(A+u) \end{pmatrix}. \quad (13)$$

Thus, the determinant and the trace of the Jacobian matrix (13) are:

$$\begin{aligned} \det(J(u, u)) &= Su^2(A+u)(u^2(2u - (1-A+M)) - AM) \\ \text{tr}(J(u, u)) &= u(((1-u)(u-M) + (u+A)(1-2u+M))u - S(A+u)), \end{aligned} \quad (14)$$

Then, the sign of the determinant (14) depends on

$$u^2(2u - (1-A+M)) - AM \quad (15)$$

and the sign of the trace (14) depends on

$$((1-u)(u-M) + (u+A)(1-2u+M))u - S(A+u). \quad (16)$$

Next, we study the stability of the positive equilibrium point  $P_1$  of system (4) with  $M < 0$  in the interior of  $\Phi$  for cases I, II and III in Table 1.

<sup>2</sup>Note that since the horizontal blow-up in (4) does not give any further information we omit the details.

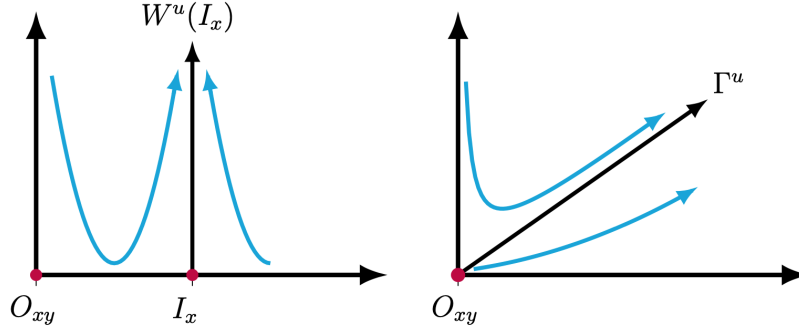


Figure 3: The panel on the left illustrates the vertical blow-up of the origin and the panel on the right illustrates the blow-down of the vertical blow up.

**Lemma 3.1.** *Let the system parameters of (4) be such that the conditions of cases I and II of Table 1 are met. Then system (4) has only one positive equilibrium point  $P_1$  which can be*

- (i) a repeller if  $S < \frac{u_1((1-u_1)(u_1-M) + (u_1+A)(1-2u_1+M))}{(A+u_1)}$ ,
- (ii) an attractor if  $S > \frac{u_1((1-u_1)(u_1-M) + (u_1+A)(1-2u_1+M))}{(A+u_1)}$ .

*Proof.* Evaluating  $u^2(2u - (1 - A + M)) - AM$  (15) at  $u_1$  gives:

$$u^2(2u - (1 - A + M)) - AM = u_1^2(2u_1 - (1 - A + M)) - AM.$$

Then,

- (i) if  $1 - A + M < 0$  then  $u_1^2(2u_1 - (1 - A + M)) - AM > 0$ . Hence  $\det(J(P_1)) > 0$  (14) since  $M < 0$ ,
- (ii) if  $1 - A + M = 0$  then  $2u_1^3 - AM > 0$ . Hence  $\det(J(P_1)) > 0$ ,
- (iii) if  $1 - A + M > 0$  then  $u_1^2(2u_1 - (1 - A + M)) - AM = u_1^3 + (A(1+M) - Q - M)u_1 - 2AM > 0$ . Hence  $\det(J(P_1)) > 0$  (14) since  $A(M+1) - Q - M \geq 0$ .

Therefore, the sign of the trace (14), and thus the behaviour of  $P_1$  in cases I and II of Table 1 depends on the parity of (16), see Figure 4.  $\square$

**Lemma 3.2.** *Let the system parameters of (4) be such that the conditions of cases III of Table 1 are met and  $\Delta > 0$  (7). Then the equilibrium point  $P_1$  is*

- (i) a saddle point if  $u_1^2(2u_1 - (1 - A + M)) - AM < 0$ ,
- (ii) a repeller if  $u_1^2(2u_1 - (1 - A + M)) - AM > 0$  and  $S < \frac{u_1((1-u_1)(u_1-M) + (u_1+A)(1-2u_1+M))}{(A+u_1)}$ ,
- (iii) an attractor if  $u_1^2(2u_1 - (1 - A + M)) - AM > 0$  and  $S > \frac{u_1((1-u_1)(u_1-M) + (u_1+A)(1-2u_1+M))}{(A+u_1)}$ .

*Proof.* Evaluating  $u^2(2u - (1 - A + M)) - AM$  (15) at  $u_1$  gives:

$$u_1^2(2u_1 - (1 - A + M)) - AM = u_1^2(2u_1 - (1 - A + M)) - AM.$$

If  $u_1^2(2u_1 - (1 - A + M)) - AM > 0$ , then the sign of the trace (14), and thus the behaviour of  $P_1$  depends on the parity of (16) at  $u_1$ , see Figure 5.  $\square$

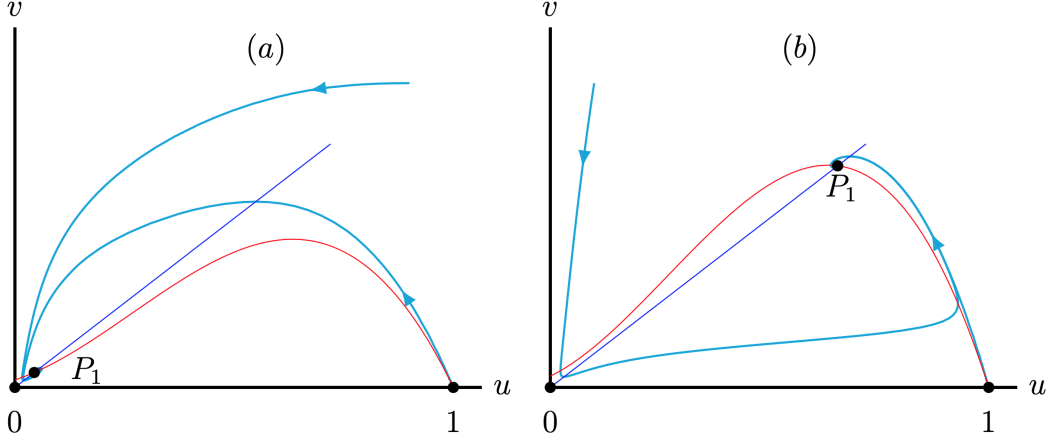


Figure 4: The blue (red) curve represents the predator (prey) nullcline. For  $A = 0.1$ ,  $M = -0.1$ ,  $S = 0.14$  and  $Q = 0.45$  (left panel) or  $Q = 0.3$  (right panel) such that system (4) has one positive equilibrium point  $P_1$  which is global attractor.

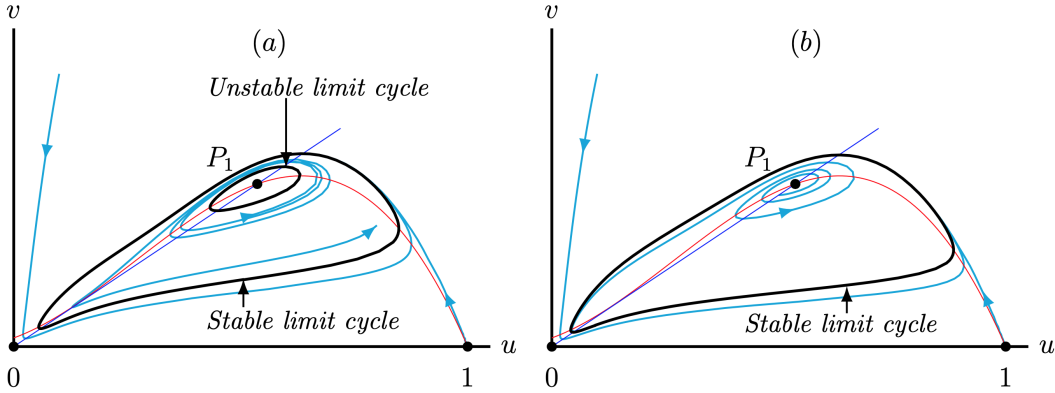


Figure 5: The blue (red) curve represents the predator (prey) nullcline. If  $A = 0.1$ ,  $Q = 0.35$ ,  $M = -0.1$  and (a)  $S = 0.159$ , then the equilibrium point  $P_1$  is attractor surrounded by two limit cycles; (b)  $S = 0.14$ , then the equilibrium point  $P_1$  is unstable surrounded by a stable limit cycles. Note that in both panel the equilibrium points  $(1, 0)$  and  $(0, 0)$  are saddle points.

**Lemma 3.3.** *Let the system parameters of (4) be such that the conditions of cases III of Table 1 are met and  $\Delta > 0$  (7). Then the equilibrium point  $P_2$  is*

(i) a saddle point if  $u_2 > u_1$ ,

(ii) a repeller if  $u_2 < u_1$  and  $S < \frac{u_2((1-u_2)(u_2-M) + (u_2+A)(1-2u_2+M))}{(A+u_2)}$ ,

(iii) an attractor if  $u_2 < u_1$  and  $S > \frac{u_2((1-u_2)(u_2-M) + (u_2+A)(1-2u_2+M))}{(A+u_2)}$ .

*Proof.* Evaluating  $u^2(2u - (1 - A + M)) - AM$  (15) at  $u_2 = (1 - A + M - u_1 - \sqrt{\Delta})/2$  gives:

$$u_2^2(2u_2 - (1 - A + M)) - AM = \frac{\sqrt{\Delta}}{4} \left( -1 - A - M + 3u_1 + \sqrt{\Delta} \right)$$

$$1 - A + M - u_1 - \sqrt{\Delta} = u_2 \sqrt{\Delta} (u_1 - u_2).$$

Then, the sign of the determinant depends on the parity of  $u_1 - u_2$ . Then, the trace (14), and thus the behaviour of  $P_2$  depends on the parity of (16) at  $u_2$ , see Figure 6.  $\square$

**Lemma 3.4.** *Let the system parameters of (4) be such that the conditions of cases III of Table 1 are met and  $\Delta > 0$  (7). Then the equilibrium point  $P_3$  is*

(i) *a saddle point if  $u_3 < u_1$ ,*

(ii) *a repeller if  $u_3 > u_1$  and  $S < u_3 \frac{((1-u_3)(u_3-M) + (u_3+A)(1-2u_3+M))}{(A+u_3)}$ ,*

(iii) *an attractor if  $u_3 > u_1$  and  $S > \frac{u_3((1-u_3)(u_3-M) + (u_3+A)(1-2u_3+M))}{(A+u_3)}$ .*

*Proof.* Evaluating  $u^2(2u - (1 - A + M)) - AM$  at  $u_3 = (1 - A + M - u_1 + \sqrt{\Delta})/2$  gives:

$$\begin{aligned} u_3^2(2u_3 - (1 - A + M)) - AM &= \frac{\sqrt{\Delta}}{4} \left( -1 + A - M + 3u_1 - \sqrt{\Delta} \right) \\ -1 + A - M + u_1 - \sqrt{\Delta} &= u_3 \sqrt{\Delta} (u_3 - u_1). \end{aligned}$$

Then, the sign of the determinant depends on the parity of  $u_3 - u_1$ . Then, the trace (14), and thus the behaviour of  $P_3$  depends on the parity of (16) at  $u_3$ , see Figure 6.  $\square$

Next, we discuss all cases when  $\Delta = 0$  and thus there exist condition for which two equilibrium points collapse, see Figure 2 and 6. In particular,

- (i) if  $P_2$  collapse with  $P_3$ , then  $P_1 < P_2 = P_3 = E_1$ ,
- (ii) if  $P_1$  collapse with  $P_2$ , then  $P_1 = P_2 = E_2 < P_3$ , and
- (iii) if  $P_2$  collapse with  $P_3$ , then  $P_2 < P_1 = P_3 = E_3$ .

As a result, the Jacobian matrix (13) reduces to

$$J(u, u) = \begin{pmatrix} Qu^2 & -Qu^2 \\ Su(A+u) & -Su(A+u) \end{pmatrix}. \quad (17)$$

Here  $\det(J(u, u)) = 0$ , so the behaviour of the equilibrium point depends on the value of the trace  $\text{tr}(J(u, u))$ . Note that as the prove for each case above are similar we only show the prove of case (i) when  $P_2$  collapse with  $P_3$ .

**Theorem 3.3.** *The equilibrium point  $P_2 = P_3 = E_1$  with*

$$E_1 = \left( \frac{1}{2}(1 - A + M - u_1), \frac{1}{2}(1 - A + M - u_1) \right)$$

is

(i) *a stable saddle-node if  $Q > \frac{S(1 + A + M - u_1)}{(1 - A + M - u_1)}$ ,*

(ii) *an unstable saddle-node if  $Q < \frac{S(1 + A + M - u_1)}{(1 - A + M - u_1)}$ .*

*Proof.* If  $\Delta = 0$ , then the equilibrium point  $P_2$  and  $P_3$  collapse and thus  $P_1 < P_2 = P_3 = E_1$ . Moreover, the determinant and the trace of the Jacobian matrix (17) at the equilibrium point  $E_1$  are

$$\begin{aligned} \det(J(E_1)) &= 0, \\ \text{tr}(J(E_1)) &= \frac{1}{4}(1 - A + M - u_1)(1 + A + M - u_1) \left( \frac{Q(1 - A + M - u_1)}{1 + A + M - u_1} - S \right). \end{aligned}$$

Therefore, the behaviour of the equilibrium point  $E_1$  depends on the value of

$$\frac{Q(1 - A + M - u_1)}{(1 + A + M - u_1)} - S.$$

$\square$

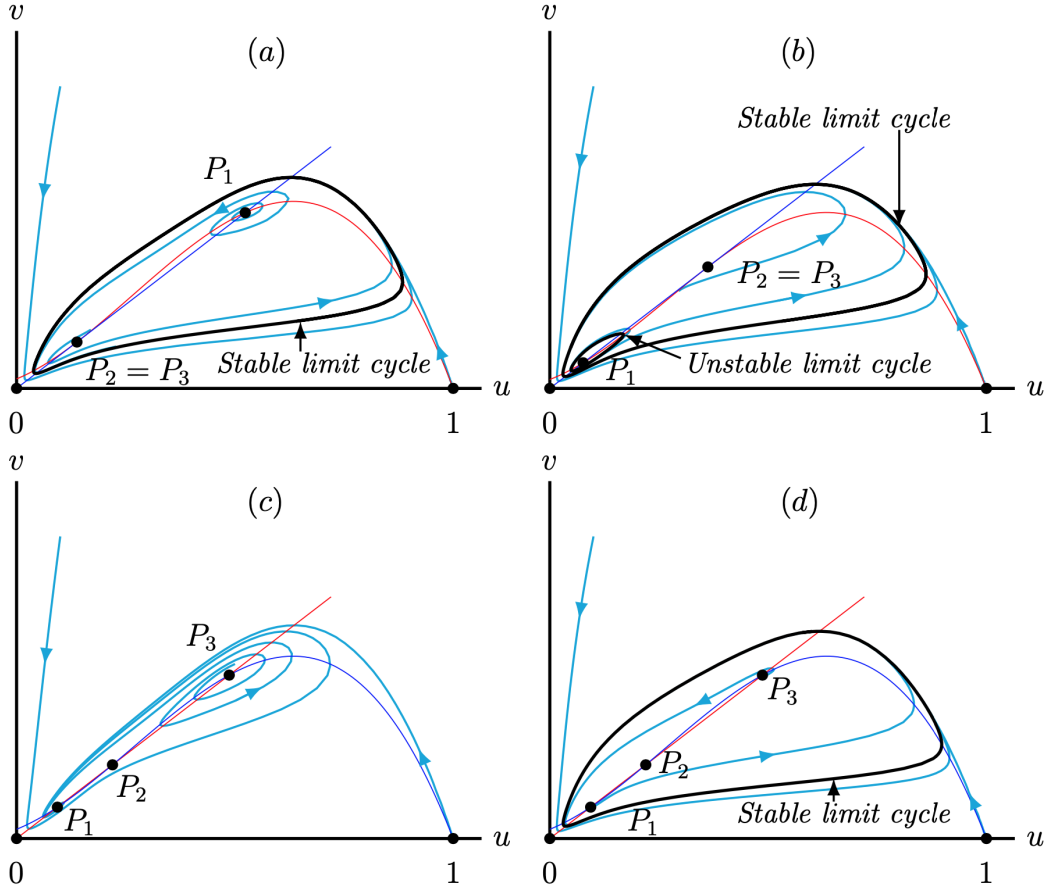


Figure 6: The blue (red) curve represents the predator (prey) nullcline. If  $A = 0.1$  and  $M = -0.1$  are fixed, then (a) for  $Q = 0.35381966$  and  $S = 0.14$  the equilibrium points  $P_2$  and  $P_3$  collapse and thus  $P_2 = P_3 < P_1$ . Additionally, the equilibrium point  $P_1$  is unstable, thus the equilibrium points  $P_2 = P_3$  and  $P_1$  are surrounded by a stable limit cycle; (b) for  $S = 0.14$  and  $Q = 0.37618034$  the equilibrium points  $P_2$  and  $P_3$  collapse and  $P_1 < P_2 = P_3$ . Moreover, the equilibrium point  $P_1$  is stable surrounded by an unstable limit cycle and thus the equilibrium points  $P_2 = P_3$  and  $P_1$  are surrounded by a stable limit cycle; (c) for  $S = 0.2$  and  $Q = 0.363$  the equilibrium point  $P_1$  is a stable node and  $P_3$  is unstable; d) for  $S = 0.13$  and  $Q = 0.363$  the equilibrium points  $P_1$  and  $P_3$  are unstable and thus the equilibrium points  $P_1, P_2$  and  $P_3$  are surrounded by a stable limit cycle.

We observe that the equation (5) does not depend on the system parameter  $S$  and thus it no affect the number of equilibrium points in the first quadrant, while the modification of  $Q$  impacts  $\Delta$  and hence the number of positive equilibrium points. If we assume the case when  $P_1 < P_2 < P_3$ , then the equilibrium point  $P_2$  is a saddle point (see Lemma 3.3) and the equilibrium points  $P_1$  and  $P_3$  are (un)stable (see Lemmas 3.2 and 3.4). Moreover, let  $W_{\downarrow}^s P_2$  be the superior stable manifold of  $P_2$  and let  $W_{\uparrow}^s P_2$  be the inferior stable manifold of  $P_2$ . Furthermore,  $W_{\downarrow}^s P_2$  and  $W_{\uparrow}^s P_2$  create a separatrix curve  $\Sigma$  in the face plane for which any solution having initial conditions above of this separatrix have the  $\omega$ -limit the point  $P_1$ . Whereas, any solutions with initial conditions under of the separatrix  $\Sigma$  have the  $\omega$ -limit the point  $P_3$ <sup>3</sup>.

In particular, we observe that the superior stable manifold of  $P_2$   $W_{\downarrow}^s P_2$  connects the boundaries of region  $\Phi$  defined in Theorem 3.1. By continuity of the vector field in  $S$ , it is clear that tthe curve determined by  $W_{\uparrow}^s(1, 0)$  remain at  $\Phi$  by Theorem 3.1 and its  $\omega$ -limit can be the point  $P_3$ , see Figure 7. Assuming that, the  $\alpha$ -limit of  $W_{\downarrow}^s P_2$  is out of  $\Phi$ , then the curve  $\Sigma$  is above the curve determined by  $W_{\uparrow}^s(1, 0)$ . If the  $\alpha$ -limit of  $W_{\downarrow}^s P_2$  is inside of  $\Phi$ , then the curve  $\Sigma$  is below the curve determined by  $W_{\uparrow}^s(1, 0)$ . Then, by By continuity of the vector field in  $S$ , there exists conditions in the  $(Q, S)$ -parameters space for which the two manifolds  $W_{\uparrow}^s(1, 0)$  and  $W_{\downarrow}^s P_2$  coincide, forming the heteroclinic curve  $\Sigma$  [37]. Furthermore, there exists  $S$  for which  $W_{\downarrow}^s P_2$  connects with  $W_{\uparrow}^u P_2$  (i.e.  $W_{\downarrow}^s P_2 \cap W_{\uparrow}^u P_2$ ) generating an homoclinic curve. Then, we have a

<sup>3</sup>Similarly, separatrix curves are clearly defined with the superior stable manifold of  $P_1$  when  $P_2 < P_1 < P_3$  and the stable manifold of  $P_3$  when  $P_2 < P_3 < P_1$ .

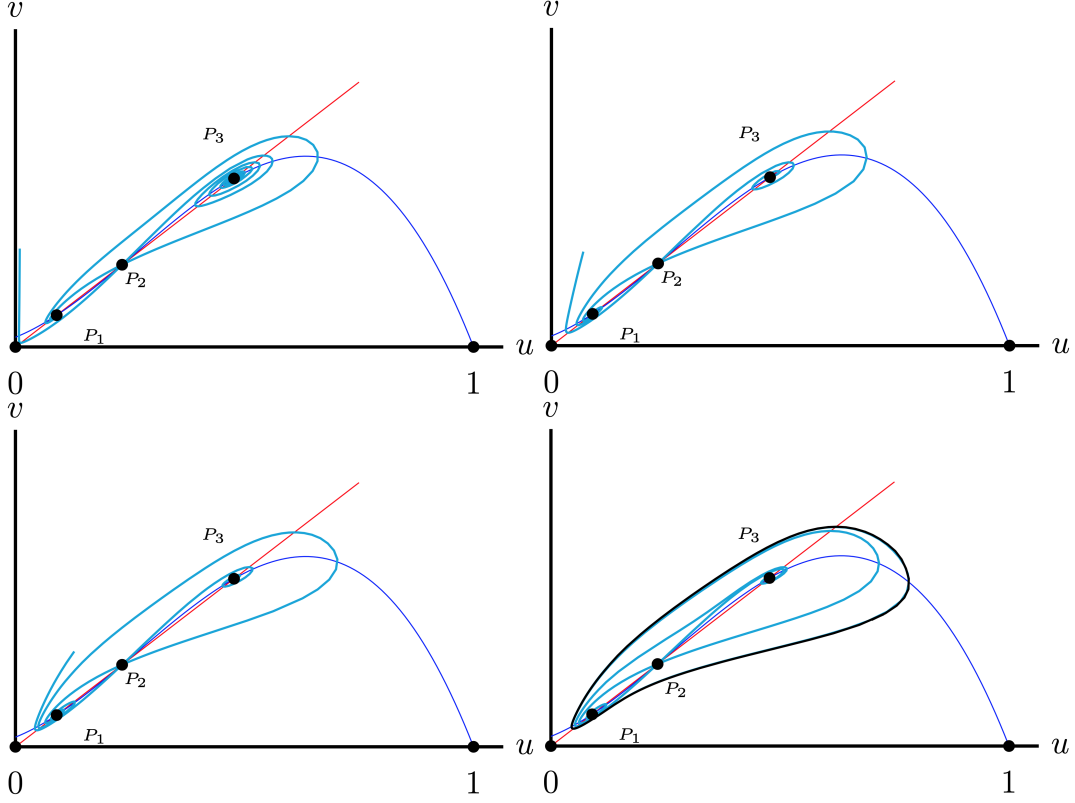


Figure 7: The stable ( $W^s P_2$ ) and unstable ( $W^u P_2$ ) manifold of the equilibrium point  $P_2$  for  $(A, M, Q) = (0.1, -0.1, 0.365)$  fixed. We observe different behaviours by continuity of the vector field in  $S$ . An animated version of this figure is accessible on <http://www.doi.org/10.6084/m9.figshare.11887830>.

non-infinitesimal limit cycle which could coincide with other limit cycle created around  $P_2$  via the Hopf bifurcation and terminates via a homoclinic bifurcation [38]. On the other hand, there exists conditions in the  $S$ -parameter space for which the equilibrium points  $P_1$  and  $P_3$  can be both unstable or one of them can be a stable equilibrium point surrounded by an unstable limit cycle or both can be a stable equilibrium points surrounded by an unstable limit cycle. Hence, the equilibrium points  $P_1$ ,  $P_2$  and  $P_3$  should be surrounded by a stable limit cycle.

## 3.2 Bifurcation Analysis

The following section will show some bifurcation analysis in the system (4) associated with the division of the parameters space. The trace and the determinant of the Jacobean matrix (17) of the system (4) are given by  $\det(J(u, u)) = 0$  and  $\text{tr}(J(u, u)) = u(Qu - S(A + u))$ . Thus, if  $Q = S(A + u)/u$  then the trace is  $\text{tr}(J(u, u)) = 0$ . Therefore, the Jacobean matrix can be written as

$$J(u, u) = \begin{pmatrix} Su(A + u) & -Su(A + u) \\ Su(A + u) & -Su(A + u) \end{pmatrix} = Su(A + u) \begin{pmatrix} 1 & -1 \\ 1 & -1 \end{pmatrix}$$

**Theorem 3.4.** *Let the system parameters be such that  $\Delta = 0$  (7) and*

$$Q = \frac{S(1 + A + M - u_1)}{(-1 + A - M + u_1)}.$$

*Then, system (4) experiences a Bogdanov–Takens bifurcation at the equilibrium point  $E_1$ <sup>4</sup>.*

<sup>4</sup>There exists conditions in the  $(Q, S)$ -parameter space for which there is another Bogdanov–Takens bifurcation when  $P_2 = P_3 < P_1$  and thus  $P_2$  and  $P_3$  collapse again.

*Proof.* If  $Q = S(1 + A + M - u_1) / (-1 + A - M + u_1)$ , then  $\det(J(E_1)) = 0$  and  $\text{tr}(J(E_1)) = 0$  and thus the Jacobian matrix of system (4) evaluated at the equilibrium point  $E_1$  simplifies to

$$J(E_1) = -\frac{1}{4}S(1 + A + M - u_1)(-1 + A - M + u_1) \begin{pmatrix} 1 & -1 \\ 1 & -1 \end{pmatrix}.$$

Now, we find the Jordan matrix form for  $J(E_1)$ , it has equal eigenvalues and a unique eigenvector  $\begin{pmatrix} 1 \\ 1 \end{pmatrix}$ . This vector will be the first column of the matrix of transformations  $\Upsilon_4$ . To obtain the second column we choose a vector that makes the matrix  $\Upsilon_4$  non-singular, in this case we take  $\begin{pmatrix} -1 \\ 0 \end{pmatrix}$ . Then:

$$\Upsilon_4 = \begin{pmatrix} 1 & -1 \\ 1 & 0 \end{pmatrix}.$$

Therefore,

$$\Upsilon_4^{-1}(J(E_1))\Upsilon_4 = \begin{pmatrix} 0 & -\frac{1}{4}S(1 + A + M - u_1)(-1 + A - M + u_1) \\ 0 & 0 \end{pmatrix}.$$

and we have the Bogdanov–Takens bifurcation or bifurcation of codimension 2 [39]. Therefore, the equilibrium point  $E_1$  is a cusp point.  $\square$

Note that the full proof of the Bogdanov–Takens bifurcation is not considered in this manuscript since the number of parameters make calculations intractable. However, it can be obtained by following [40] and [39] where the authors showed that their system undergoes to a Bogdanov–Takens bifurcation by unfolding the system around the cusp of codimension two. Nowadays, there are several computational methods to find Bogdanov–Takens points. These methods are implemented in software packages such as MATCONT [41]. Figure 8 illustrates two Bogdanov–Takens bifurcation which was detected with MATCONT in the  $(Q, S)$ -plane for  $(A, M)$  fixed.

**Theorem 3.5.** *Let the system parameters be such that  $\Delta = 0$  (7). Then, system (4) experiences a saddle-node bifurcation at the equilibrium point  $E_1$  (similarly for the saddle-node bifurcation at the equilibrium points  $E_2$  when  $P_1 = P_2$  and  $E_3$  when  $P_1 = P_3$ ).*

*Proof.* We will prove that the system (4) has a saddle-node bifurcation at

$$Q = \frac{S(1 + A + M - u_1)}{(1 - A + M - u_1)}$$

based on Sotomayor’s theorem [42]. For  $\Delta = 0$  the points  $P_2$  and  $P_3$  collapse and  $P_1 < P_2 = P_3$ . Thus, there are two equilibrium points in the first quadrant. Those are  $P_1$  and  $E_1 = (1 - A + M - u_1) / 2$ .

The Jacobian matrix of the system (4) evaluate at the equilibrium point  $E_1$  is

$$J(E_1) = \begin{pmatrix} \frac{Q(-1 + A - M + u_1)^2}{4} & -\frac{Q(-1 + A - M + u_1)^2}{4} \\ \frac{S(1 + A + M - u_1)(-1 + A - M + u_1)}{4} & -\frac{S(1 + A + M - u_1)(-1 + A - M + u_1)}{4} \end{pmatrix}.$$

Moreover, setting the dynamical system (4) by a vector form given by

$$f(u, v; Q) = \begin{pmatrix} (u + A)(1 - u)(u - M) - Qv \\ u - v \end{pmatrix}. \quad (18)$$

It is clear to see that  $\det(J(E_1)) = 0$ . Let

$$V = \begin{pmatrix} v_1 \\ v_2 \end{pmatrix} = \begin{pmatrix} 1 \\ 1 \end{pmatrix}$$

the eigenvector corresponding to the eigenvalue  $\lambda = 0$  of the matrix  $J(E_1)$ . Additionally, let

$$U = \begin{pmatrix} u_1 \\ u_2 \end{pmatrix} = \begin{pmatrix} \frac{S(1 + A + M - u_1)}{Q(-1 + A - M + u_1)} \\ 1 \end{pmatrix}$$

the eigenvector corresponding to the eigenvalue  $\lambda = 0$  of the matrix  $(J(E_1))^T$ .

On the other hand, differentiating the the vector function (18) with respect to the bifurcation parameter  $Q$  we obtain

$$f_Q(u, v, Q) = \begin{pmatrix} \frac{-1 + A - M + u_1}{2} \\ 0 \end{pmatrix}.$$

Therefore,

$$U \cdot f_Q(u, v; Q) = \frac{S(1 + A + M - u_1)}{2Q} \neq 0.$$

Now we analyse the expression  $U \cdot D^2 f(u, v; Q)(V, V)$  where  $V = (v_1, v_2)$  and  $D^2 f(u, v; Q)(V, V)$  is

$$\begin{aligned} D^2 f(u, v; Q)(V, V) &= \frac{\partial^2 f(u, v; Q)}{\partial u^2} v_1 v_1 + \frac{\partial^2 f(u, v; Q)}{\partial u \partial v} v_1 v_2 + \frac{\partial^2 f(u, v; Q)}{\partial v \partial u} v_2 v_1 + \frac{\partial^2 f(u, v; Q)}{\partial v^2} v_2 v_2 \\ &= \begin{pmatrix} -2(2 + A - M) \\ 0 \end{pmatrix}. \end{aligned}$$

Thus,

$$U \cdot D^2 f(u, v; Q)(V, V) = -\frac{2S(2 + A - M)(1 + A + M - u_1)}{Q(-1 + A - M + u_1)} \neq 0.$$

Therefore, by Sotomayor's theorem the system (4) has a saddle-node bifurcation at  $E_1$ . Note that the saddle-node bifurcation at the equilibrium points  $E_2$  (when  $P_1 = P_2$ ) and  $E_3$  (when  $P_1 = P_3$ ) can be obtained following in the same way that we proved the saddle-node bifurcation at  $E_1$ .  $\square$

We consider the case when the positive equilibrium points are  $P_1 < P_2 < P_3$  to explain the dynamics of the bifurcation diagram. However, there are two other cases where two of those points can collapse and then disappear, i.e  $P_1 < P_2 = P_3$  or  $P_2 = P_3 < P_1$ . The bifurcation curves obtained from Theorem 3.5 and 3.4 divide the  $(Q, S)$ -parameter-space into twelve regions, see Figure 8. From our results we observe that for  $A, M$  fixed and modifying the parameter  $Q$  impacts the number of positive equilibrium points of system (4). While, the modification of the parameter  $S$  changes the stability of the positive equilibrium points  $P_1$  and  $P_3$  of system (4), while the other equilibrium points  $(0, 0)$ ,  $(1, 0)$  and  $P_2$  do not change their behaviour. When parameters lie in the curve  $Q = Q^*$  the equilibrium points  $P_2$  and  $P_3$  collapse and we have  $P_1 < P_2 = P_3$ . In addition, when parameters lie in the curve  $Q = Q^{**}$  the equilibrium points  $P_2$  and  $P_3$  collapse again and now we have  $P_2 = P_3 < P_1$ . Thus, system (4) has conditions for a saddle-node bifurcation and Bogdanov–Takens bifurcation. Moreover, when the parameters be located in Region I and VIII, system (4) has one positive equilibrium point which is always a stable node. When the parameters moved to Regions II and XII system (4) has one equilibrium points that is an unstable node surrounded by a stable limit cycle. In addition, when the parameters lie in Regions III and IX  $P_1$  and  $P_3$  are stable. Furthermore, when the parameters lie in Regions IV  $P_1$  is stable,  $P_3$  is stable surrounded by an unstable limit cycle. When the parameters lie in Regions V  $P_1$  is stable and  $P_3$  is unstable node. When the parameters lie in Regions VI,  $P_1$  is stable surrounded by an unstable limit cycle and  $P_3$  is unstable node. When the parameters  $Q$  and  $S$  are located in Region VII  $P_1$  and  $P_3$  are unstable and thus the equilibrium points are surrounded by a stable limit cycle. In region X,  $P_1$  is stable and  $P_3$  is unstable, so the equilibrium points are again surrounded by a stable limit cycle. Finally, when the parameters be located in Region XI, system (4) has one equilibrium points that is a stable node surrounded by two limit cycle.

## 4 Conclusions

In this manuscript, we study the Leslie–Gower predator-prey model with weak Allee effect (i.e system (2) with  $m < 0$ ) and functional response Holling type II. We simplify the analysis by studying a topologically equivalent system (4). The topologically equivalent system (4) has two equilibrium points in the axis which are always saddle points. Whereas, system (4) can has at most three positive equilibrium point in the first quadrant, see Figures 1 and 2. Moreover, we prove that equilibrium points  $P_1$ ,  $P_2$  and  $P_3$  can be saddle and/or (un)stable points. In addition, when there are three equilibrium points in the first quadrant one of them (the middle point) is always a saddle point. The stable manifold of the saddle equilibrium point determines a separatrix curve which divides the basins of attraction between the other two equilibrium points, see Figure 7.

As the function  $\varphi$  is a diffeomorphism preserving the orientation of time, the dynamics of system (2) is topologically equivalent to system (4) [29, Theorem 1]. Therefore, we can conclude that there are conditions in the system parameter for which the predator and prey can coexist or both populations oscillate. This behaviour depends on the predation rate ( $q$ ) and the intrinsic growth rate of the predator ( $s$ ).

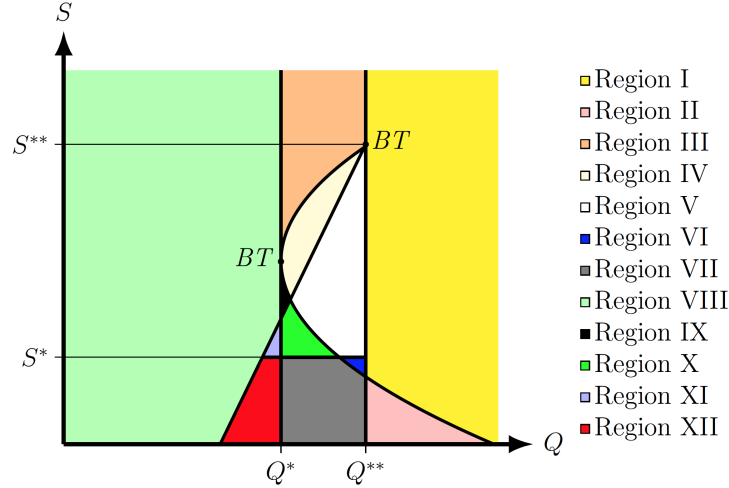


Figure 8: The bifurcation diagram of system (4) for  $(A, M) = (0.1, -0.1)$  fixed and created with the numerical bifurcation package MATCONT [41]. The curve  $H$  represents the Hopf curve,  $SN_{1,2}$  represents the saddle-node curve, and  $BT$  represents the Bogdanov–Takens bifurcation.

We showed that the weak Allee effect in the Leslie–Gower model (2) better represent the dynamics of the original Leslie–Gower predator-prey model studied, for example, by Saez and Gonzalez-Olivares [35]. From [35], we can conclude that species in system (1) could coexist or oscillate but could not extinct. Since there is always one positive equilibrium point which can be stable, or unstable surrounded by a stable limit cycle, or stable surrounded by two limit cycles.

This manuscript complements the results of the Leslie–Gower model studied by Courchamp *et al.* [27] in which the prey is affected by a density-dependent phenomenon. We showed the impact in the stabilisation and oscillation of the species by considering the weak Allee effect in the prey for two parameters which are the rescaled intrinsic growth rate of the predator and the predation rate, see Figure 8.

In summary, the bifurcation diagram of the Leslie–Gower model (2) (see Figure 8) is often qualitatively similar with the bifurcation diagram of the original model (1) but their solutions behave quantitatively different. In other words, it is observed that the model support equivalent ecological behaviour due to the addition of the modifications into the Leslie–Gower model. That is, a strong Allee effect ( $m > 0$ ) support coexistence and extinction of the species. In contrast, the original model and the model with weak Allee effect ( $m < 0$ ) does not support the extinction of the species.

## References

- [1] C. Arancibia-Ibarra. The basins of attraction in a Modified May–Holling–Tanner predator-prey model with Allee effect. *Nonlinear Analysis: Theory, Methods & Applications*, 185:15–28, 2019.
- [2] S. Kundu and S. Maitra. Asymptotic behaviors of a two prey one predator model with cooperation among the prey species in a stochastic environment. *Journal of Applied Mathematics and Computing*, pages 1–27, 2019.
- [3] N. Martínez-Jeraldo and P. Aguirre. Allee effect acting on the prey species in a Leslie–Gower predation model. *Nonlinear Analysis: Real World Applications*, 45:895–917, 2019.
- [4] R. Mateo, A. Gastón, M. Aroca-Fernández, O. Broennimann, A. Guisan, S. Saura, and J. García-Viñas. Hierarchical species distribution models in support of vegetation conservation at the landscape scale. *Journal of Vegetation Science*, 30:386–396, 2019.
- [5] A. Mondal, A. Pal, and GP. Samanta. On the dynamics of evolutionary Leslie-Gower predator-prey eco-epidemiological model with disease in predator. *Ecological Genetics and Genomics*, 10:1–12, 2019.
- [6] X. Santos and M. Cheylan. Taxonomic and functional response of a Mediterranean reptile assemblage to a repeated fire regime. *Biological Conservation*, 168:90–98, 2013.
- [7] P. Turchin. *Complex population dynamics: a theoretical/empirical synthesis*, volume 35 of *Monographs in population biology*. Princeton University Press, Princeton, N.J., 2003.

- [8] D. Hooper, F. Chapin, J. Ewel, A. Hector, P. Inchausti, S. Lavorel, J. Lawton, D. Lodge, M. Loreau, and S. Naeem. Effects of biodiversity on ecosystem functioning: a consensus of current knowledge. *Ecological monographs*, 75:3–35, 2005.
- [9] R. May. *Stability and complexity in model ecosystems*, volume 6 of *Monographs in population biology*. Princeton University Press, Princeton, N.J., 1974.
- [10] A.P. Moller, B.G. Stokke, and D.S.M. Samia. Hawk models, hawk mimics, and antipredator behavior of prey. *Behavioral Ecology*, 26:1039–1044, 2015.
- [11] R. Monclus, D. von Holst, D. Blumstein, and H. Rödel. Long-term effects of litter sex ratio on female reproduction in two iteroparous mammals. *Functional ecology*, 28:954–962, 2014.
- [12] I. Hanski, H. Henttonen, E. Korpimäki, L. Oksanen, and P. Turchin. Small-rodent dynamics and predation. *Ecology*, 82:1505–1520, 2001.
- [13] I. Hanski, L. Hansson, and H. Henttonen. Specialist predators, generalist predators, and the microtine rodent cycle. *The Journal of Animal Ecology*, pages 353–367, 1991.
- [14] P. Roux, J. Shaw, and S. Chown. Ontogenetic shifts in plant interactions vary with environmental severity and affect population structure. *New Phytologist*, 200:241–250, 2013.
- [15] M. Bimler, D. Stouffer, H. Lai, and M. Mayfield. Accurate predictions of coexistence in natural systems require the inclusion of facilitative interactions and environmental dependency. *Journal of Ecology*, 106:1839–1852, 2018.
- [16] S. Wood and M. Thomas. Super-sensitivity to structure in biological models. *Proceedings of the Royal Society of London. Series B: Biological Sciences*, 266:565–570, 1999.
- [17] I. Graham M and X. Lambin. The impact of weasel predation on cyclic field-vole survival: the specialist predator hypothesis contradicted. *Journal of Animal Ecology*, 71:946–956, 2002.
- [18] C. Baker, A. Gordon, and M. Bode. Ensemble ecosystem modeling for predicting ecosystem response to predator reintroduction. *Conservation biology*, 31:376–384, 2017.
- [19] R. Levins. Discussion paper: the qualitative analysis of partially specified systems. *Annals of the New York Academy of Sciences*, 231:123–138, 1974.
- [20] B. Raymond, J. McInnes, J. Dambachera nd S. Way, and D. Bergstrom. Qualitative modelling of invasive species eradication on subantarctic Macquarie Island. *Journal of Applied Ecology*, 48:181–191, 2011.
- [21] C. S. Holling. The components of predation as revealed by a study of small mammal predation of the European pine sawfly. *Tenth International Congress of Entomology*, 91:293–320, 1959.
- [22] F. Courchamp, T. Clutton-Brock, and B. Grenfell. Inverse density dependence and the Allee effect. *Trends in Ecology & Evolution*, 14:405–410, 1999.
- [23] W. Allee, O. Park, A. Emerson, T. Park, and K. Schmidt. *Principles of animal ecology*. WB Saundere Co. Ltd., Philadelphia, 1949.
- [24] L. Berec, E. Angulo, and F. Courchamp. Multiple Allee effects and population management. *Trends in Ecology & Evolution*, 22:185–191, 2007.
- [25] P. Stephens and W. Sutherland. Consequences of the Allee effect for behaviour, ecology and conservation. *Trends in Ecology & Evolution*, 14:401–405, 1999.
- [26] P. Stephens, W. Sutherland, and R. Freckleton. What is the Allee effect? *Oikos*, 87:185–190, 1999.
- [27] F. Courchamp, L. Berec, and J. Gascoigne. *Allee effects in ecology and conservation*. Oxford University Press, 2008.
- [28] R. Ostfeld and C. Canham. Density-dependent processes in meadow voles: an experimental approach. *Ecology*, 76:521–532, 1995.
- [29] C. Arancibia-Ibarra, J. Flores, G. Pettet, and P. van Heijster. A Holling–Tanner predator–prey model with strong Allee effect. *International Journal of Bifurcation and Chaos*, 29(11):1–16, 2019.
- [30] C. Arancibia-Ibarra and E. González-Olivares. A modified Leslie–Gower predator–prey model with hyperbolic functional response and Allee effect on prey. *BIOMAT 2010 International Symposium on Mathematical and Computational Biology*, pages 146–162, 2011.
- [31] E. González-Olivares, L. Gallego-Berrío, B. González-Yañez, and A. Rojas-Palma. Consequences of weak Allee effect on prey in the May–Holling–Tanner predator–prey model. *Mathematical Methods in the Applied Sciences*, 38:5183–5186, 2015.
- [32] E. González-Olivares, J. Mena-Lorca, A. Rojas-Palma, and J. Flores. Dynamical complexities in the Leslie–Gower predator–prey model as consequences of the Allee effect on prey. *Applied Mathematical Modelling*, 35:366–381, 2011.

- [33] P. Tintinago-Ruíz, L. Restrepo-Alape, and E. González-Olivares. Consequences of Weak Allee Effect in a Leslie–Gower-Type Predator–Prey Model with a Generalized Holling Type III Functional Response. In *Analysis, Modelling, Optimization, and Numerical Techniques*, pages 89–103. Springer, 2015.
- [34] F. Dumortier, J. Llibre, and J. Artés. *Qualitative theory of planar differential systems*. Springer Berlin Heidelberg, Springer-Verlag Berlin Heidelberg, 2006.
- [35] E. Sáez and E. González-Olivares. Dynamics on a predator–prey model. *SIAM Journal on Applied Mathematics*, 59:1867–1878, 1999.
- [36] A. Andronov. *Qualitative theory of second-order dynamic systems*, volume 22054. Halsted Press, 1973.
- [37] C. Chicone. *Ordinary Differential Equations with Applications*, volume 34 of *Texts in Applied Mathematics*. World Scientific, Springer-Verlag New York, 2006.
- [38] V. Gaiko. *Global Bifurcation Theory and Hilbert’s Sixteenth Problem*, volume 562 of *Mathematics and Its Applications*. Springer Science & Business Media, 2013.
- [39] D. Xiao and S. Ruan. Bogdanov–Takens bifurcations in predator–prey systems with constant rate harvesting. *Fields Institute Communications*, 21:493–506, 1999.
- [40] J. Huang, Y. Gong, and S. Ruan. Bifurcation analysis in a predator-prey model with constant-yield predator harvesting. *Discrete and Continuous Dynamical Systems Series B*, 18:2101–2121, 2013.
- [41] A. Dhooge, W. Govaerts, and Y. Kuznetsov. Matcont: a matlab package for numerical bifurcation analysis of odes. *ACM Transactions on Mathematical Software (TOMS)*, 29:141–164, 2003.
- [42] L. Perko. *Differential Equations and Dynamical Systems*. Springer New York, 2001.